This is a repository copy of *Mobile Multi-Gigabit Visible Light Communication System in Realistic Indoor Environment*.

White Rose Research Online URL for this paper:
http://eprints.whiterose.ac.uk/89030/

Version: Accepted Version

Article:

Mobile Multi-gigabit Visible Light Communication System in Realistic Indoor Environment

Ahmed Taha Hussein and Jaafar M.H. Elmirghani

School of Electronic and Electrical Engineering, University of Leeds, LS2 9JT, United Kingdom
{ml12ath, j.m.h.elmirghani}@leeds.ac.uk

Abstract—**The main challenges facing high data rate visible light communication (VLC) are the low modulation bandwidth of the current transmitters (i.e. light emitting diodes, LEDs), the inter symbol interference (ISI) caused by multipath propagation and co-channel interference (CCI) due to multiple transmitters. In this paper, for the first time, to best of our knowledge, we propose, design and evaluate the use of laser diodes (LDs) for communication as well as illumination. In addition, we propose an imaging receiver for a mobile VLC system to mitigate ISI. A novel delay adaptation technique is proposed to mitigate CCI, maximise the signal to noise ratio (SNR) and reduce the impact of multipath dispersion under user mobility. The proposed imaging system is able to provide data rates of 5 Gbps in the worst case scenario. The combination of a delay adaptation approach with an imaging receiver (DAT imaging LD-VLC system) adds a degree of freedom to the link design, which results in a VLC system that has the ability to provide higher data rates (i.e. 10 Gbps) in the considered harsh indoor environment. The proposed technique (delay adaptation) achieves significant improvements in the VLC channel bandwidth (more than 16 GHz) over imaging system in a worst case scenario. The VLC channel characteristics and links were evaluated under diverse situations including an empty room and a room with very strong shadowing effects resulting from mini cubicle offices.**

Index Terms— *Laser diodes, imaging receiver, multi-gigabit VLC system, delay adaptation, real environment.*

I. INTRODUCTION

Traditional radio and microwave communication systems suffer from limited channel capacity and transmission rate due to the limited radio spectrum available. Concurrently, the data rates requested by users continue to increase exponentially. There is a potential band of the electromagnetic spectrum (i.e. optical band) available that is able to provide tens of Gbps for users in the near future [1] especially for indoor users. Visible light communication (VLC) systems are among the promising solutions to the bandwidth limitation problem faced by radio frequency systems [2]. Significant research effort is being directed towards the development of VLC systems due to their numerous advantages over radio systems, such as: 1) the nature of light gives the VLC system immunity against interference caused by adjacent channels with the possibility of frequency reuse in different parts of the same building, which means abundant capacity; 2) the VLC system also offers better security at the physical layer, and this is due to the fact that light does not penetrate through opaque barriers, which means there is no eavesdropping possible as with radio systems; 3) the availability of simple front-end devices at low cost; 4) energy efficient system due to its dual functionally (i.e. illumination and communication); 5) hundreds of THz of license-free bandwidth; 6) harmless for humans and other electronic devices; and 7) easy to integrate into the existing lighting infrastructure. There are however several challenges hindering the development of VLC systems. These challenges include the low modulation bandwidth of the light emitting diodes (LEDs) and inter symbol interference (ISI). Significant efforts are being directed towards finding solutions for the VLC system limitations. Among the most notable solutions is the use of pre or post equalization (or both) [3], complex multiple access and modulation techniques [4], [5] and parallel communication (optical multiple input multiple output-OMIMO) [6]. The modulation bandwidth available in the transmitters (LEDs) is typically less than the VLC channel bandwidth, which means that the former limits the transmission rates.

The main VLC system achievements using LEDs are presented in the following. A blue optical filter at the receiver is used to filter the slow response yellowish component, and this technique is considered to be the simplest and most cost effective approach to increase data rates [7]. However, the achieved bandwidth is insignificant (8 MHz). The drop in the white LED response can be compensated for by using a simple analogue pre-equalization at the transmitter side, and this technique can offer 40 Mbps without the use of a blue filter [8]. However, the data rate achieved is still very low compared to the VLC spectrum. A moderate data rate (80 Mbps) can be achieved using more complex pre-equalization [3]. But, pre-equalization has the drawback that the drive circuit for the LED needs to be modified, and this leads to higher costs and lower efficiency of the emitter (i.e. not all input power is converted to the light). By combining a simple pre and post equalization, 75 Mbps can be achieved [9]. A speed of 100-230 Mbps was the maximum data rate achieved using phosphorescent LEDs with simple On-Off keying (OOK) modulation [10]. Higher data rates can be achieved when complex modulation approaches are used, for example, Discrete Multi-tone modulation (DMT) can provide data rates of about 1 Gbps [4]. However, this type of modulation technique requires a complex transceiver. In terms of parallel transmission, a VLC system is the optimal choice for optical MIMO, as many LEDs (transmitters) are used for illumination and can send different data streams on every single LED to maximise the throughput. At the same time, an array of photo detectors are necessary at the receiver side, and this setup offers improvements in security, link range and data range while the power required is unaltered [6]. A real enhancement in the data rates can be achieved with red, green and blue (RGB) LEDs. A 1.25 Gbps was reported in [11] when using RGB LEDs in a single colour transmission mode, and 1.5 Gbps has been achieved by using a new design of μLED array, and it uses non-return-to-zero OOK (NRZ-OOK) as a modulation scheme. The 3 dB modulation bandwidth of this LED was 150 MHz [12]. The maximum data rate has been achieved by using commercial RGB LEDs with low complexity modulation (OOK) was up to 500 Mbps [13]. Recently, a 3 Gbps VLC system based on a single

1

μLED using orthogonal frequency division multiplexing (OFDM) has been successfully demonstrated [14]. The highest throughput achieved by LEDs was reported in [5], which reported an aggregate throughput of 3.4 Gbps using DMT, wavelength division multiplexing (WDM) and RGB LEDs. The design and implementation complexity are a major concern in these systems.

Recent research has suggested that laser diodes (LDs) can provide more-efficient lighting than LEDs. A prototype laser-based headlight system was demonstrated by the car maker BMW. This system uses blue lasers and phosphors to generate white light [15]. A prototype from Sandia lab proved that by using four colour laser sources it could provide a practical white light illumination source [16]. In their experiment, four laser diodes were used (red, green, yellow and blue) to generate white light that was similar to that from other light sources, such as incandescent lights and white LEDs [16]. Lasers were not expected to be ideal light sources because of their extremely narrow line-width and extremely narrow spot size. However, the results from using four-colour laser sources have shown experimentally that the colour rendering quality of the white light is good, and this paved the way for serious consideration of the use of lasers in solid state lighting [16]. One of the main potential issues associated with using laser lighting is that lasers can be dangerous to human eyes. Therefore, it should be noted that while the original sources indeed have laser source properties (colours red, green, yellow and blue), once they have been combined and had the beam scattered and diffused, the light no longer has the characteristics of laser light, but resembles white light [17], [18]. In 2011, Toshiba launched LDs lighting that achieves much higher luminance within a much smaller area, and it can be used for various applications that require much higher luminous flux (it produces 4500 lumens using 90 Watts) than available with conventional white LEDs [19]. Recently, different types of RGB-LD lights were investigated to generate white light, blue lasers in combination with yellow emitting YAG:Ces and RGB lasers resulted in a luminous flux of 252 lumens and luminous efficacy of 76 lm/W was reported in [20].

Various techniques have been proposed to combat ISI in VLC systems. The authors in [21] proposed a return-to-zero OOK (RZ-OOK) modulation, with the space between pulses being used as a guard to reduce the effect of the delay in low data rate applications; while, in [22] they used OFDM techniques to mitigate the ISI effect. A spread spectrum has also been considered to combat ISI, however, it reduces the bandwidth efficiency as well [23]. The authors in [24] used zero forcing (ZF) equalization with such transmitter (i.e. LED) arrangements to reduce the effects of ISI. The achieved bit error rate (BER) with this technique was similar to the channel without ISI.

In this paper, we introduce for the first time LDs as a source of illumination and communication for a VLC system in conjunction with two different receivers (wide field of view (FOV), and imaging). The main goal of using LDs is to enable the VLC system to achieve multi-gigabits when employing a simple modulation technique (OOK), and thus adding simplicity to the VLC system. In addition, an imaging receiver was proposed for a VLC system instead of wide FOV receiver to mitigate the impact of ISI, reduce the delay spread (increase the channel bandwidth) and increase the signal to noise ratio (SNR) when the VLC system operates at high data rates (5 Gbps) under the effects of mobility and multipath dispersion.

In a mobile indoor VLC system the distance between the LDs' light units and the receiver is a key factor; thus, sending the information signals from all LDs units at the same time increases the delay spread that decreases the 3 dB channel bandwidth. To further enhance the communication links and to provide higher data rates (beyond 5 Gbps) with the imaging LD-VLC system, a novel beam delay adaptation technique coupled with imaging LD-VLC system (DAT imaging LD-VLC system) to mitigate the ISI, co-channel interference (CCI) due to multiple transmitters and reduce the impact of multipath dispersion due to mobility at the receiver is proposed here. Instead of transmitting the signals at the same time from different LD light units, the proposed algorithm sends the signal that has the longest journey first, and then it sends the other signals with different differential delays (Δt) so that all the signals reach the receiver at the same time. To ensure that all the transmissions reach the receiver at the same time, the beam delay adaptation technique introduces a differential delay (Δt) between the transmissions.

We also model two different room scenarios: an empty room and a real environment room that has a door, windows, bookshelves, mini cubicles and other objects. The difficulty related with all two room arrangements is the ability to establish LOS communication link between transmitter (i.e. LD light unit) and receiver at all possible locations. The results showed an enhancement in channel bandwidth from 4.2 GHz to 23 GHz when the imaging LD-VLC system was combined with our algorithm in a worst case scenario (i.e. real environment). In addition, the proposed system (i.e. DAT imaging LD-VLC system) has ability to maintain strong LOS component in a harsh realistic environment in all receiver locations which lead to receive high optical power in addition to reduce multipath dispersion. Our results indicate that the DAT imaging LD-VLC system achieves significant 3 dB channel bandwidth enhancements over imaging and wide FOV systems when realistic environment is exist.

The reminder of this paper is divided into sections as follows: Section II introduces the design of the LDs light based on illumination engineering. Section III shows laser VLC system and rooms setup. Section IV presents receivers configurations. Simulation results and discussions about the use of LDs in conjunction with wide FOV and imaging receivers in an empty room are presented in Section V. Section VI describes the delay adaptation technique; and the simulation results and discussion of the delay adaption technique in an empty room are presented in Section VII. The robustness of the proposed adaptive systems against mobility, shadowing and signal blockage is investigated in Section VIII. Finally, conclusions are drawn in Section IX.

II. LDs Light Design

To achieve comfortable office lighting, a certain amount of illumination is required. According to European standard EN 12464-1, illumination should be at least 300 lx in an office [25]. Assuming that the LD light has a Lambertian radiation pattern, the direct LOS illumination at a point (x, y) in the floor of the room can be estimated as shown in the following [26], [27]:

$$E_{LOS} = I(0) \frac{cos^n(\theta) \, cos(\gamma)}{D_1^2} \qquad (1)$$

where $I(0)$ is the centre luminous intensity of the LD, θ is the irradiance angle, D_1 is the distance between the LD and any point in the floor, γ is the angle of incidence and n is the Lambertian emission order as defined in [28]:

$$n = -\frac{ln(2)}{ln\left(cos\left(\Phi_{\frac{1}{2}}\right)\right)} \qquad (2)$$

where $\Phi_{\frac{1}{2}}$ is the semi angle at half power of the LD. Then the first reflection of illumination can be defined as shown in the following [29], [30]:

2

$$E_{FST} = \frac{I(0)\,cos^n(\theta)\,cos(\gamma)cos(\vartheta)\,cos(\delta)d_{A1}\rho_1}{\pi D_1^2 D_2^2} \qquad (3)$$

where D_1 is the distance from the LD light to the first element, D_2 is the distance from the first element to the floor, d_{A1} is the area of the element in the first reflection, ρ_1 is the reflection coefficient, ϑ and δ are the angles of irradiance and incidence for the elements respectively. The second reflection of illumination can be calculated as [29], [30]:

$$E_{SEC} = \frac{I(0)\,cos^n(\theta)\,cos(\gamma)cos(\vartheta)\,cos(\delta)cos(\beta)cos(\emptyset)d_{A1}d_{A2}\rho_1\rho_2}{\pi^2 D_1^2 D_2^2 D_3^2} \qquad (4)$$

where D_1 is the distance from the LD light to the first element, D_2 is the distance from first element to second element, D_3 is the distance from the second element to the floor, d_{A2} is the area of the second element in the second reflection, ρ_2 are the reflection coefficients, β and $\emptyset$ are the angles of irradiance and incidence for the second element respectively. The total horizontal illumination at any point in the floor can be calculated as follows:

$$E_t = \sum_1^f E_{LOS} + \sum_1^k E_{FST} + \sum_1^r E_{SEC} \qquad (5)$$

where f is the number of LD light units, k is the number of reflecting elements in the first reflection and r is the number of reflecting elements in the second reflection.

III. Laser VLC System and Rooms Setup

To study the benefits of our techniques for an indoor VLC system, a simulation based on a ray-tracing algorithm was performed in two room configurations. The simulation model was developed using room dimensions of 4m×8m (width×length) with a ceiling height of 3 m, and the room configurations were denoted as room (A) and room (B). Figs.1 (a) and (b) show room A, which is an empty room, and room B, which is a realistic environment as normally experienced in office arrangements where a door, windows, furniture and mini cubicles block the optical signal. Both rooms experience multipath propagation. Given typical indoor walls and floor colours and textures, typical reflection coefficients of 0.3 for the floor and 0.8 for the walls and ceiling were used for room A [31], [32]. These relatively high reflectivities (within the typically range) were selected as they result in the greatest multipath dispersion (worst case scenario), and consequently considerable pulse spread. Fig. 1 (b) shows room B which has three large windows, a door, bookshelves, furniture, chairs and cubicles that have surfaces parallel to the walls of the room. These objects can create shadowing. In room B, the door and three glass windows were assumed to not reflect any signal; therefore, their diffuse reflectivities were set to zero. Moreover, the walls and the ceiling have a diffuse reflectivity of 0.8 and the floor has a 0.3 diffuse reflectivity. Two of the walls: x=4m (excluding the door) and y =8m were covered by filling cabinets and bookshelves with diffuse reflectivity of 0.4. It was assumed that signals encountering a physical barrier were either blocked or absorbed. Additionally, desks, tables and chairs inside room B have similar reflectivities to the floor (i.e. 0.3). The complexity is distinct in room B where low reflectivity objects and physical partitions can create significant shadowing and signal blocking.

Experimental measurements of plaster walls have shown that they are roughly a Lambertian reflector [31]. Therefore, all the walls, the ceiling and the floor in rooms A and B were modelled as Lambertian reflectors with high reflectivity. To model the reflections, the room was divided into a number of equally sized squares with an area of dA and reflection coefficient of ρ. Each reflection element was treated as a small transmitter that transmits an attenuated version of the received signals from its

centre in a Lambertian pattern with n =1 (Lambertian source has $\Phi = 60^o$).

Previous research considered only LOS and reflections up to a first order [11], [21], [29]. However, this may not provide a full description of the characteristics of the system. Therefore, in this work reflections up to second order were considered, since the second reflection can have a great impact on the system performance (especially at high data rates). To ensure computations can be performed within a reasonable time, surface elements of size 5 cm × 5 cm for first-order reflections and 20 cm × 20 cm for second-order reflections were used. In our evaluation channel characteristics, optical power received, delay spread, 3 dB channel bandwidth, and path-loss calculations were determined in similar way to that used in [28], [32].

The simulations and calculations reported in this paper were carried out using the MATLAB program. Our simulation tool is similar to one developed by Barry *et al.* [33], and is used to produce impulse responses, the power distribution and to calculate the delay spread, 3 dB channel bandwidth and SNR.

A combination of red, green and blue lasers with a diffuser can be used to generate white light that has good colour rendering [34]. Therefore, the room's illumination was provided by eight RGB-LD light units which were used to ensure that ISO and European standards were satisfied [25]. Each LD light unit has 9 (3×3) RGB-LD. The LD lights were installed at a height of 3 m above the floor. The specifications of the RGB-LDs used in this study were adapted from the practical results reported in [16], where the measured illuminace for each RGB-LD was 193 lx. Therefore, the centre illumination intensity for each RGB-LD was 162 cd. The conversion from illuminace (lx) to luminous intensity (cd) was carried out using the inverse square law which is valid if (i) the source is a point source (ii) the beam is divergent and (iii) distance of interest is greater than ten times of the source size [35]. Fig.2 shows the architecture of the LD light units, where the light from three lasers (i.e. RGB) is combined using beam combiners, then passes through multiple ground glass diffusers to reduce speckle before illuminating the room. This design is similar to the one studied in [16]. Beam-splitters and detectors were used to monitor and control (tune LDs light engine) the different laser powers. A few percent of the beam power is needed for that purpose. Changing the power emitted by each laser can be used to obtain the exact colour desired and set the total emitted power. A number of different uniformly distributed LD light unit configurations (i.e. 4, 6 and 8 LD units) were tested to find the optimum number of units that ensure that the ISO and EU standards illumination requirements are satisfied in the room. We found that eight units were the optimum for illumination, and we used this in our study; four and six light units in the room did not achieve the minimum illumination requirement (i.e. 300 lx [25]). The height of the work desks where the transmitters and receivers associated with the user equipment are placed was 1m. This horizontal plane was referred to as the "communication floor", (CF), Figs. 1a and 1b. Fig.3 shows the horizontal illumination distributions from the eight RGB-LD light units at the CF level. It is clear from this figure that there is sufficient illumination according to EU and ISO standards [25].

In optical wireless (OW) links including VLC system, intensity modulation with direct detection (IM/DD) is the preferred choice [28], [36]. IM can be simply defined as the instantaneous power of the optical carrier modulated by the signal. At the receiver side, DD is used to generate electrical current proportional to the instantaneous received optical power. An indoor OW channel that uses IM/DD can be fully characterised by the impulse response ($h(t)$) of the channel as given in [37]:
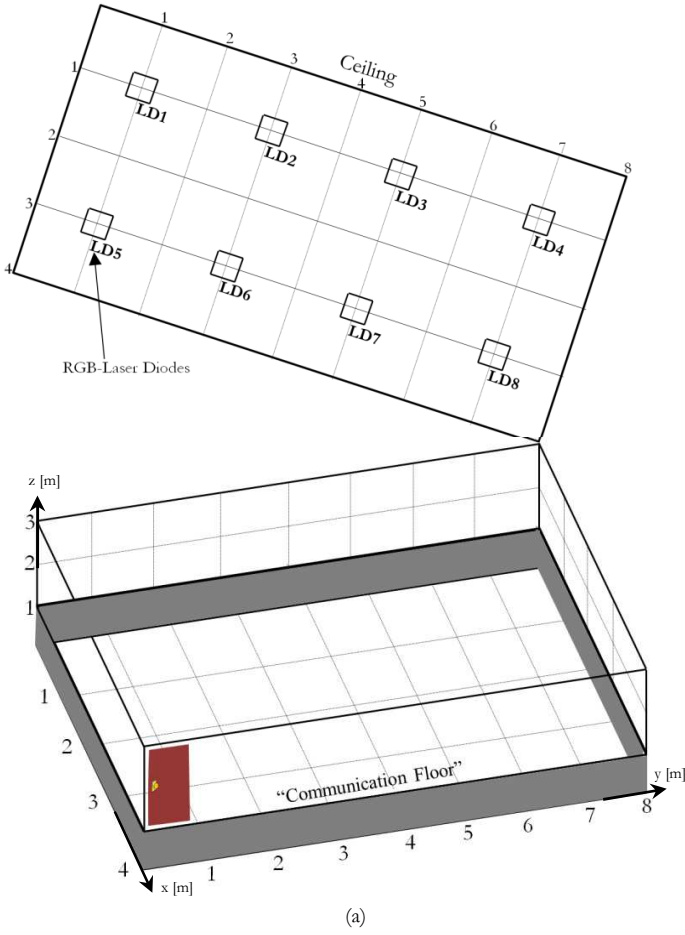
3

Fig.1: VLC system rooms (a) an empty room (Room A) and (b) a realistic room which has a door, three large glass windows a number of rectangular-shaped cubicles with surfaces parallel to the room walls (Room B).
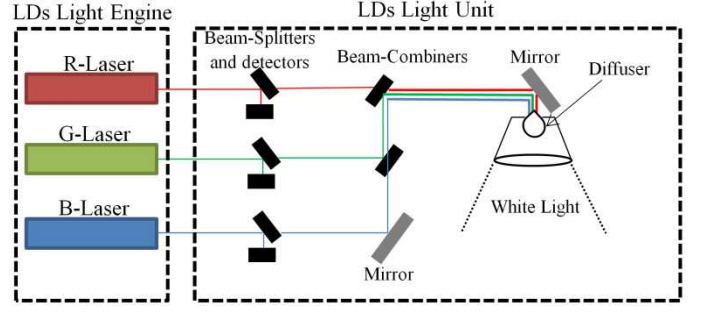

Fig.2: Architecture of RGB-LD white light; light from three lasers is combined using chromatic beam-combiners, then passes through multiple ground glass diffusers to reduce speckle before illuminating the room.
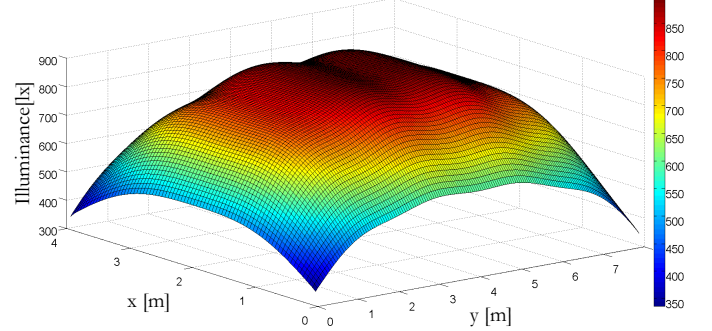

Fig.3: Distribution of horizontal illumination at the communication floor, Min. 336 lx and Max. 894 lx.

$$I(t, Az, El) = \sum_{s=1}^{S} Rx(t) \otimes h_m(t, Az, El) + RN_b \tag{6}$$

where $I(t, Az, El)$ is the received instantaneous photocurrent in the photo-detector with photo-detector responsivity (R) using S elements to receive a transmitted signal $x(t)$ through channel h in the presence of AWGN (N_b). Az and El are the direction of arrival in the azimuth and elevation angles, t is the absolute time and $\otimes$ denotes convolution. The VLC signal emitted by the RGB-LD reaches the receiver through various paths of different lengths. These propagation paths change with the receiver movement, and/or the movement of the surrounding objects. However, the paths are fixed for a given fixed configuration. The channel impulse response can be represented approximately as the sum of scaled and delayed Dirac delta functions [28]. A simulation package based on a ray-tracing algorithm was developed in order to compute the impulse response on the entire communication floor. The channel impulse response can be given as:

$$h(t) = \sum_{k=0}^{\infty} h^{(k)}(t) \tag{7}$$

where $h(t)$ is the impulse response due to the LOS and reflection components. As previously mentioned, in this study up to second-order reflections are considered, and therefore k takes values of 0, 1, and 2. Several parameters can be obtained by simulating the VLC impulse response, such as 3 dB channel bandwidth and delay spread. Indoor OW systems are subjected to multipath dispersion due to non-directed transmission, which can cause ISI. Delay spread is a good measure of signal pulse spread due to the temporal dispersion of the incoming signal. The delay spread of an impulse response is given by:

$$D = \sqrt{\frac{\sum (t_i - \mu)^2 P_{ri}^2}{\sum P_{ri}^2}} \tag{8}$$

where t_i is the delay time associated with the received optical power P_{ri} and μ is the mean delay given by:

$$\mu = \frac{\sum t_i P_{ri}^2}{\sum P_{ri}^2} \tag{9}$$

4

IV. Receivers Configurations

We used two types of receivers, an imaging receiver, and a non-imaging receiver with one wide FOV (FOV = $90°$) element with photo sensitive area of 1 cm². The latter is the most basic receiver configuration widely investigated in previous research [28], [29], [31]. In contrast, the imaging receiver employs multiple pixels with narrower FOV. Narrow FOVs were chosen for the pixels to limit the range of optical rays (representing different path lengths) received hence limiting the ISI at high data rates and supporting mobility. The imaging receiver presents two potential advantages over non-imaging wide FOV receiver: firstly, a single planner array is used for all photo-detectors, which can facilitate the use of a large number of pixels. Secondly, a common imaging concentrator (for example, a lens) can be shared among all photo-detectors, reducing the cost and size compared to other kinds of receivers [38]. The photocurrents received in each pixel can be amplified separately and can be processed using different methods such as select the best (SB) or maximum ratio combining (MRC) techniques to maximise the power efficiency of the system [39]. The detector array of the imaging receiver is segmented into J equal-sized rectangular shaped pixels as shown in Fig.4. In this case, and under most circumstances, the signal falls on no more than four pixels [40]. Therefore, the area of each pixel is the photo-detector's area, which is equal to the exit area of the imaging concentrator used, divided by the number of pixels. In this paper the detector array was segmented into 50 pixels and the imaging receiver employed an imaging concentrator. The transmission factor of the concentrator is given by [38]:

$$T_c(\delta) = -0.1982\delta^2 + 0.0425\delta + 0.8778 \tag{10}$$

where δ is the incidence angle measured in radians. We set the semi acceptance angle (ψ_a) of this concentrator to $65°$ so that it can view the whole ceiling when the receiver is at the centre of the room. In this work, the photo detector array of the imaging receiver was segmented into 50 pixels (5 rows and 10 columns). When the receiver is at the centre of the room it is designed to see the whole ceiling, therefore the ceiling was subdivided in this case into 50 segments (5×10) along the x and y axes respectively, and each reception area or segment is cast onto a single pixel. The entrance area of the imaging receiver was $A = \frac{9\pi}{4}$ cm², while the exit area was $A' = \frac{A\sin^2(\psi_a)}{N^2}$, where N is the refractive index (N = 1.7). The concentrator gain ($g(\psi a)$) is be given by [28]:

$$g(\psi a) = \frac{N^2}{\sin^2(\psi_a)} \tag{11}$$

The detector array is assumed to fit exactly into its corresponding concentrator's exit area. Therefore, the detector array has a photosensitive area of 2 cm² and each pixel has an area of 4 mm². In our design, each reception area is cast onto a single pixel when the receiver is at the centre of the room. A pixel's reception area can be found by calculating the reception angles α_x and α_y with respect to the receiver's normal along the x and y directions as shown in Fig.5. α_x and α_y can be calculated by $\alpha_x = tan^{-1}\left(\frac{d_x}{h}\right)$ and $\alpha_y = tan^{-1}\left(\frac{d_y}{h}\right)$, where d_x and d_y are the x-axis and y-axis horizontal separations and h is the reception area height [40]. In addition, the reception area observed by each pixel varies as the imaging receiver moves (the new reception area

should be calculated when the receiver moves). These reception angles (α_x and α_y) become a design property (reference points) of the imaging receiver at all locations. At certain locations on the CF, some of the reception areas on the ceiling start to appear on one of the walls, when the receiver is located at the room corner, as shown in Fig.6. The height of the centre of the reception area above the CF, Z_y or Z_x on the xz-wall or the yz-wall, respectively, can be calculated by:

$$Z_y = \left(\frac{Y_r}{tan\,\alpha_y}\right) \text{ and } Z_x = \left(\frac{X_r}{tan\,\alpha_x}\right) \tag{12}$$

where Y_r and X_r are the horizontal separation distances between the imaging receiver and the xz-wall and yz-wall respectively.
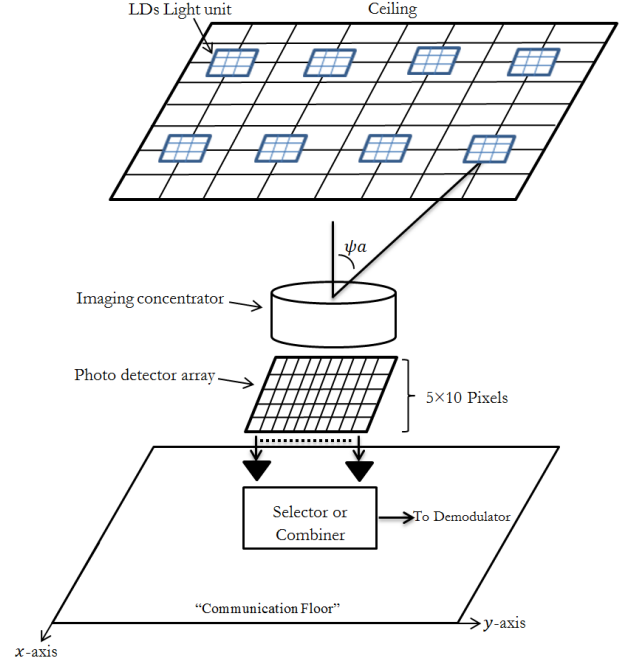

Fig.4: Imaging receiver [41], [42] physical structure of an imaging receiver which uses a single imaging lens with a photo-detector segmented into multiple pixels.
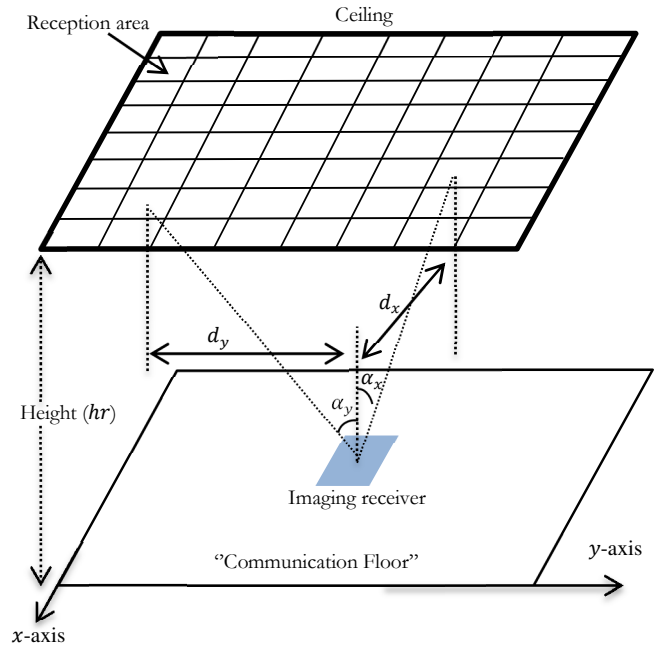

Fig.5: Reception area distribution associated with the photo-detector array when the receiver is placed at the centre of the room.
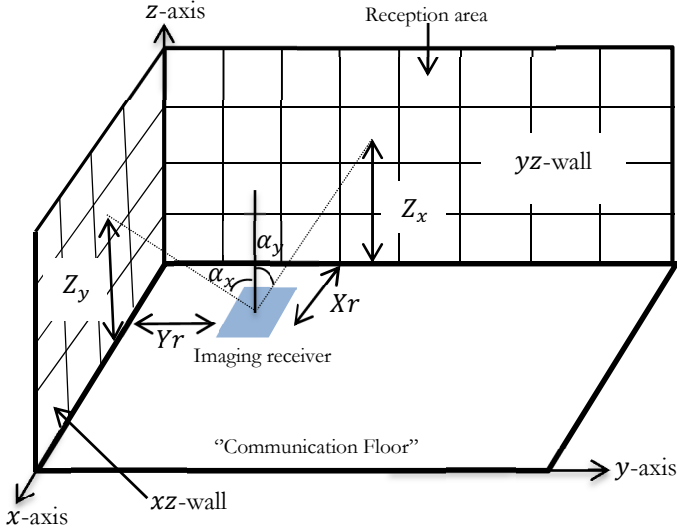
5

Fig.6: Reception area distribution associated with the photo-detector array when the receiver is placed at the corner of the room.

The impulse responses and magnitude responses of the two receivers (wide FOV and imaging receivers) at the room centre are depicted in Fig.7. From this figure it can be clearly seen that the imaging receiver's impulse response (Fig.7 b) is better than that of the wide FOV receiver in terms of signal spread. The impulse response of the wide FOV receiver (Fig.7 a) contains many peaks that correspond to different direct LOS components coming from different LD light units. The impulse response of the wide FOV receiver also shows that the LOS as well as first and second reflection components have a great impact on the signal, because these components cause the signal to spread over a large time-range (see Fig.7 a), which is due to the wide FOV's of this receiver. From Fig.7 (b) we can see that the first and the second reflections were significantly reduced when using the imaging receiver at this location, which means the ISI was almost eliminated. In addition, the power received by the imaging receiver was too low (6.7 μW for single pixel and 34.8 for all pixels) compared to the wide FOV receiver (345 μW) as shown in Fig.7 (b). This difference in received power between the imaging receiver and wide FOV receiver is due to three reasons: 1) the concentrator acceptance angle in the imaging receiver is 65° which reduces the number of rays accepted (to reduce ISI) 2) the narrow FOV of each pixel (about 21°) also restricts the number of rays and hence the overall received power 3) the photo detector area for each pixel is 4 mm² while the wide FOV receiver has 1 cm² area with 90° FOV. However, when SNR is calculated (see equation 14) most of the received power in the wide FOV receiver contributes to P_{s0} (powers associated with logic 0) due to dispersion in the signal received by the wide FOV receiver, which leads to ISI. In the practical VLC system, the impulse response is continuous, but the simulator subdivides the reflecting surfaces into discrete elements. We have tried to reduce the effect of discretisation by grouping power with time in a bin so it was equal to a 0.01 ns duration as a single received power. A good choice of time bin should be equal or less than $\sqrt{dA}/c$ [33], which is roughly the time light takes to travel between neighbouring elements. It should be noted that reducing dA leads to improved resolution in the impulse response evaluation together with an increase in the computation time exponentially.

V. RESULTS AND DISCUSSIONS

In this section, we evaluated the performance of the proposed LD-VLC system using wide FOV and imaging receivers in an empty room in the presence of multipath dispersion and mobility. The proposed systems are examined within fourteen different locations when all the receivers move along the y-axis. The results are presented in terms of delay spread, 3 dB channel bandwidth and SNR. Due to the symmetry of the room, the results for x=3 equal the results for x=1, therefore only x=1m and x=2m results are shown along the y-axis.

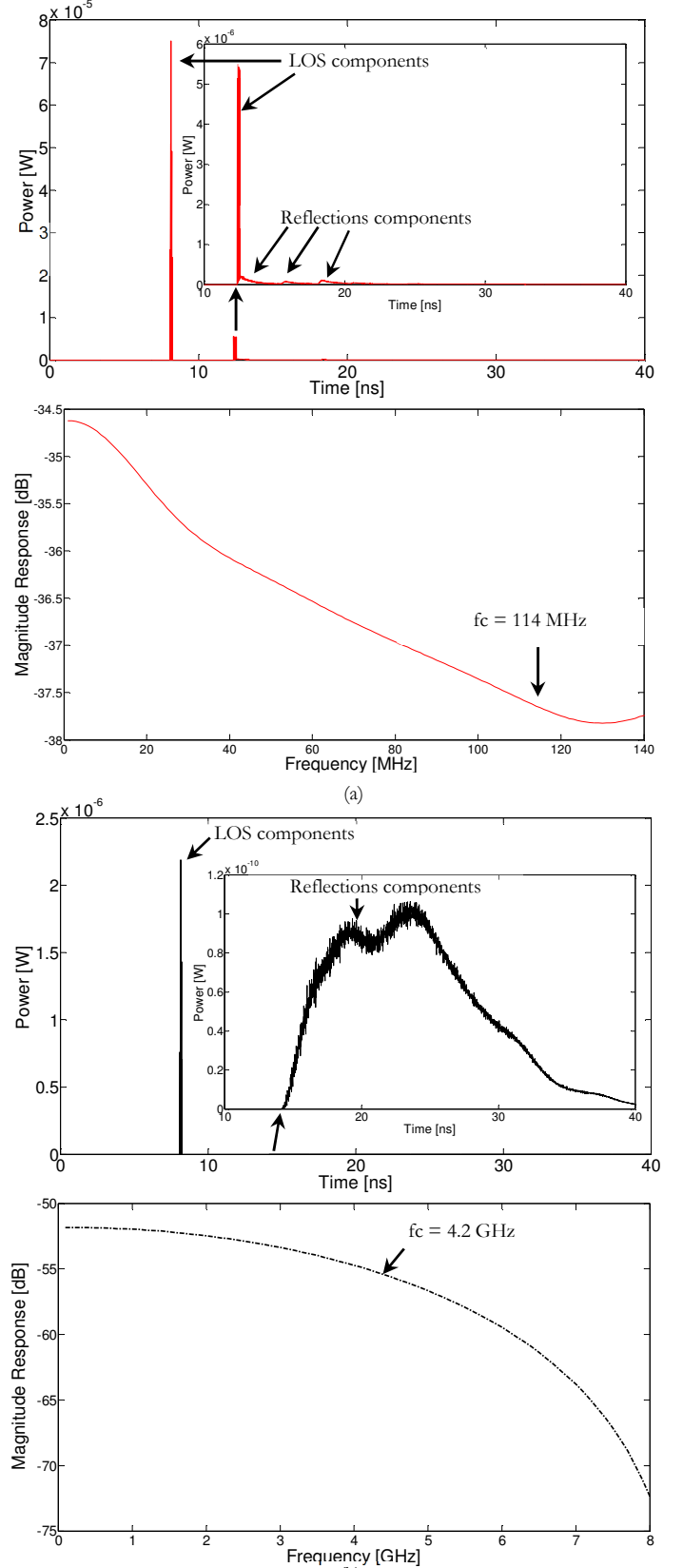

Fig.7: Impulse and frequency responses of the two receivers, (a) wide FOV receiver (b) imaging receiver at room centre (x=2m, y=4m, z=1m).

6

A. Delay Spread

Fig.8 presents the communication system delay spread associated with the wide FOV LD-VLC and imaging LD-VLC systems. The results show that the imaging LD-VLC system has lower delay spread compared to the wide FOV LD-VLC system at all the receiver locations considered. In the imaging LD-VLC system, the results indicate that employing an image receiver instead of a wide FOV receiver can reduce the delay spread by a factor of 17 in our system (operated in a typical room) from 0.7 ns to 0.04 ns at the worst communication path (centre of the room, (x=2m, y=4m)). This improvement is due to the limited range of the rays accepted by the small pixels with narrow FOV. The variation in delay spread along the x=1m and x=2m is due to the dominance of the direct line of sight component under a VLC light source and its weakness at locations between VLC light sources. Further reduction in delay spread can be achieved when our delay adaptation technique is used in conjunction with the imaging receiver.
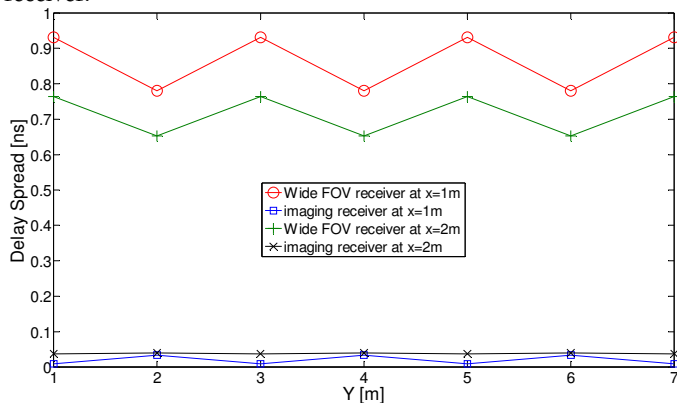

Fig.8: Delay spread of the wide FOV and the imaging LD-VLC systems in fourteen different locations when all the receivers move along the y-axis.

B. 3 dB Channel Bandwidth

Although, the transmitter modulation bandwidth problem in the VLC system can be solved by replacing LEDs with LDs, the channel bandwidth remains an issue that needs to be tackled to achieve multi-gigabits. We dealt with channel bandwidth (the second problem) by using an imaging receiver instead of a wide FOV receiver. The 3 dB channel bandwidth achieved by the two receivers is shown in Fig.9, note the variation in channel bandwidth in tandem with the delay spread due to the effects explained. The results show that the imaging receiver provides a larger bandwidth compared to the traditional wide FOV receiver. The minimum communication channel bandwidth of the wide-FOV receiver was 70 MHz at x=1m and y=1m (worst communication path for the wide FOV receiver due to high multipath propagation). In contrast, the minimum channel bandwidth in the imaging LD-VLC system was 4.2 GHz at x=2m and y=4m (this value enables a data rate of up to 6 Gbps [43]). This increased channel bandwidth enables the VLC system to operate at higher data rates while using a simple modulation technique, (OOK) [44]. The imaging LD-VLC system produced significant improvements in the channel bandwidth at all receiver locations compared to the wide FOV system. This is attributed to reducing the contribution of the reflection components by using a narrow FOV pixel and by appropriately weighing (MRC fashion) the pixels' contributions resulting in an emphasis on the direct power component (i.e. LOS). For instance, at the least successful receiver location (x=2m and y=4m), a significant bandwidth enhancement can be achieved, a factor of 36 (from 116 MHz to 4.2 GHz), when our imaging LD-VLC is used instead of the wide

FOV LD-VLC system. To the best of our knowledge, this is the highest channel bandwidth and data rates reported for an indoor mobile VLC system with simple modulation format and system design. Also, it should be noted that the results in Fig.8 are in agreement with the general observation made in Fig.9. For instance, in the imaging system at the point x=1m and y=1m the delay spread is lowest resulting in the highest channel bandwidth (Fig.9). Similar agreement is observed when comparing other locations. In an optical direct detection system, the optimum receiver bandwidth is 0.7 times the bit rate. Therefore, the maximum data rate that can be achieved by a wide FOV receiver is 100 Mbps due to the channel bandwidth being 70 MHz. The 0.7 figure is based on Personick's optical receiver design [43].
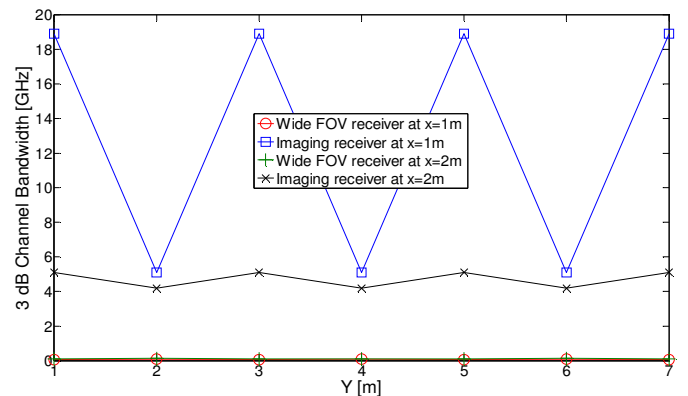

Fig.9: 3 dB channel bandwidth of the wide FOV and the imaging LD-VLC systems in fourteen different locations when all the receivers move along the y-axis.

C. SNR Analysis

Indoor VLC communication systems are strongly impaired by ISI and mobility. The conventional OOK-BER of the indoor VLC system can be given as [37]:

$$BER = \frac{1}{2} \, erfc\left(\sqrt{SNR/2}\right) \qquad (13)$$

where $erfc$ is the complementary error function. In this paper we consider two methods of processing the electrical signal (SB and MRC) from different pixels in the imaging receiver. In the SB technique the receiver simply selects the pixel with the largest SNR among all the pixels. The SNR_{SB} is given by [37]:

$$SNR_{SB} = Max_i\left(\frac{R(P_{s1}-P_{s0})}{\sigma_t}\right)^2 \qquad 1 \le i \le j \qquad (14)$$

where j=50 when the imaging receiver is used, R is the receiver responsivity (0.4 A/W) and P_{s1} and P_{s0} are the powers associated with logic 1 and 0 respectively. σ_t is the total variance noise that is the sum of shot noise, thermal noise and shot noise associated with the received signal. N can be calculated as [37]:

$$\sigma_t = \sqrt{\sigma_{shot}^2 + \sigma_{preamplifier}^2 + \sigma_{signal}^2} \qquad (15)$$

where σ_{shot}^2 represents the background shot noise component, $\sigma_{preamplifier}^2$ represents the preamplifier noise component and σ_{signal}^2 represents the shot noise associated with the received signal. In this paper, for the bit rate of 30 Mbps we used the p-i-n FET [38] and p-i-n BJT trans-impedance preamplifier [45] receivers. Higher data rates of 5 Gbps and 10 Gbps are also considered, and here we used the p-i-n FET receivers designed in [46], [47]. The input noise current was 4.5 pA/$\sqrt{Hz}$ for the 5 GHz receiver and 10 pA/$\sqrt{Hz}$ for the 10 GHz respectively [46], [47]. The MRC approach utilises all pixels in the imaging receiver. The output signals of all the pixels are combined through an adder circuit. Each input to the circuit is added with a

7

weight proportional to its SNR to maximise the SNR. The SNR_{MRC} is given by [37]:

$$SNR_{MRC} = \left(\frac{\left(\sum_{i=1}^{j} R(P_{s1i} - P_{s0i}) W_i \right)^2}{\sum_{i=1}^{j} \sigma_t^2 W_i^2} \right) \quad (16)$$

where W_i is the weight of each pixel $\left(\frac{R(P_{s1} - P_{s0})}{\sigma_t^2} \right)$. Then the SNR_{MRC} can be written as [37]:

$$SNR_{MRC} = \left(\frac{\left(\sum_{i=1}^{j} R(P_{s1i} - P_{s0i}) \left(\frac{R(P_{s1} - P_{s0})}{\sigma_t^2} \right) \right)^2}{\sum_{i=1}^{j} \sigma_t^2 \left(\frac{R(P_{s1} - P_{s0})}{\sigma_t^2} \right)^2} \right)$$

$$= \sum_{i=1}^{j} \frac{(R^2 (P_{s1i} - P_{s0i})^2)}{\sigma_t^2} = \sum_{i}^{j} SNR_i \quad (17)$$

Significant improvement in the SNR was achieved at 30 Mbps when the imaging LD-VLC system was used instead of the wide FOV LD-VLC system. It can be clearly seen that the imaging receiver achieves about 3 dB SNR gain over the wide FOV receiver when the SB technique was applied and about 8 dB when the MRC technique was applied at the centre of the room (x=2m and y=4m), which represents the worst communication paths for the imaging receiver (SNR gain is higher in other locations as shown in Fig.10). In the VLC systems, the impact of ISI is larger than other noise components, typically up to 20 Gbps [29]. Therefore, significant improvements can be achieved by using an imaging receiver at high data rates. This significant improvement in the SNR level is attributed to the ability of the imaging receiver to collect the VLC signal with minimum ISI, due to its narrow FOV pixels and large overall detection area provided by the large number of pixels.

To evaluate the performance of the imaging system at higher bit rates, the SNR was calculated at 5 Gbps. Fig.11 illustrates the SNR of the imaging system when it operated at 5 Gbps; the imaging LD-VLC system achieved about 16.1 dB SNR when using the SB approach and approximately 19.1 dB SNR at the room centre when using MRC. This means that the bit error rate (BER) provided by our imaging system is better than 10^{-9} at 5 Gbps. It should be noted that an MRC imaging system outperforms an SB imaging system. SB is a simple form of diversity, where the receiver simply selects the pixel with the largest SNR among all the pixels. In contrast, MRC utilises all the pixels in the imaging receiver and combines the output signals from the pixels with weights dictated by the SNR observed by each pixel. A pixel that observes a better SNR is given a higher weight. Therefore SB is a subset of MRC and the MRC receiver is as such comparable to or better than SB as our results show. In Fig.9 the 3 dB channel bandwidth achieved by the wide FOV receivers does not enable them to transfer data at a rate of 5 Gbps, therefore, we only present results for the imaging receiver at high data rates (i.e. 5 Gbps).

VI. DELAY ADAPTATION TECHNIQUE (DAT)

All the LD units typically emit signals simultaneously, which means the signal from the closest LD light unit reaches the receiver first before signals from distant LD units, and this causes co-channel interference (CCI) which leads to significant induced performance degradation. To reduce the impact of this impairment we proposed a delay adaptation technique coupled with an imaging receiver (imaging receiver eliminates the effect of ISI) to enhance the SNR and system bandwidth. To ensure that all the transmissions reach the receiver at the same time, our beam delay adaptation technique introduces a differential delay (Δt) between the transmissions. It should be noted that DAT cannot be employed in a straight forward fashion with VLC

systems when employing MIMO transmission. This technique can be easily applied when all VLC transmitters send same information signal at the same time.
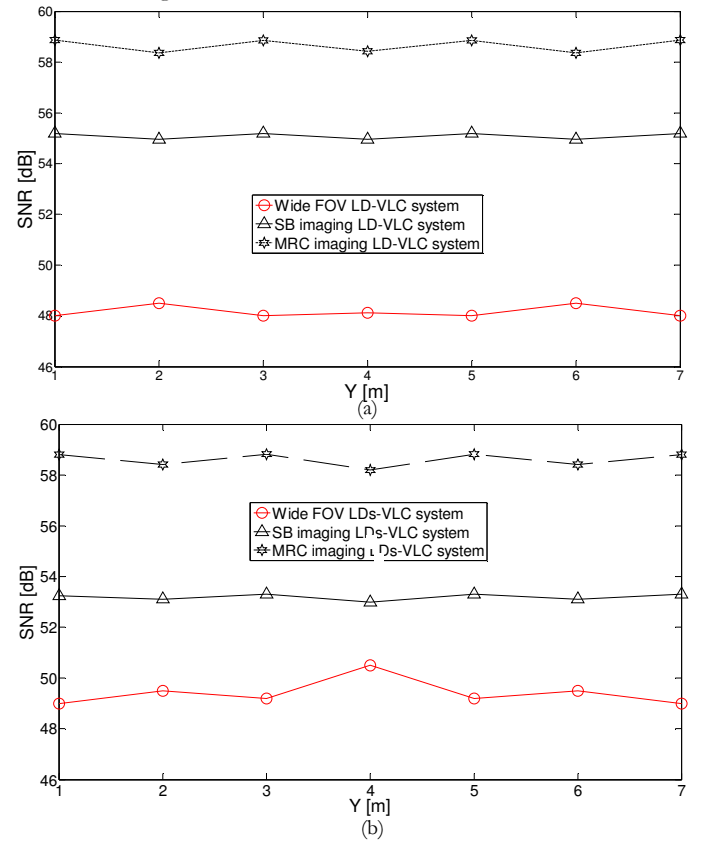

Fig.10: SNR of the two systems operating at 30 Mbps and using two combing schemes (SB and MRC for imaging receiver), (a) at x=1m and (b) at x=2m along the y-axis.
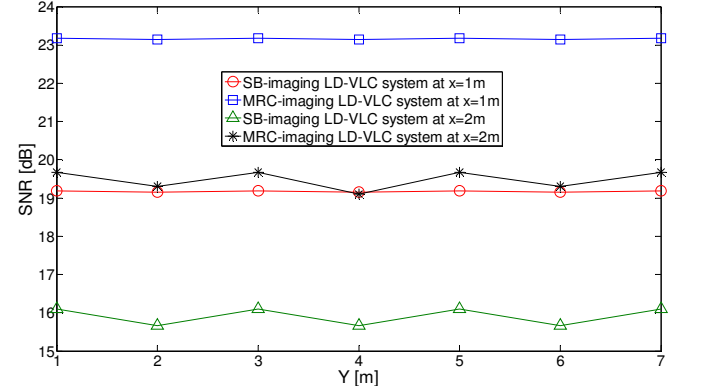

Fig.11: SNR of imaging LD-VLC system operating at 5 Gbps and using two combing schemes (SB and MRC), at x=1m and at x=2m along the y-axis.

The delay adaptation adjusts the transmission times of the signals as follows:

1- Send a pilot signal from the first RGB-LD unit to calculate the mean delay (μ) at the receiver for this RGB-LD unit.
2- Repeat step 1 for all pixels in the imaging receiver (the aim of this step is to find the best pixel that has the lowest mean delay (μ) among all pixels).
3- Repeat steps 1 and 2 for all RGB-LD units.
4- The receiver calculates the differential delays (Δt) between the received pulses from each of the RGB-LD units.
5- The receiver uses an infrared beam at a low data rate to send a control feedback signal to inform all the transmitters of the delays associated with each

8

transmitter (eight delay values relayed to each transmitter in the case of our 2 rooms in Fig.1 that have eight RGB-LD units).

6- The transmitters send signals from the RGB-LD units in an ascending order according to the delay values such that a RGB-LD unit that has the largest delay, i.e. longest path to the receiver transmits first.

A speed of 1 m/s is typical for indoor users [48], we therefore propose that the receiver re-estimates its delay values for all LD light units at the start of a 1 second frame and if these have changed compared to the previous frame values then the receiver uses the feedback channel to update the transmitters. If the time taken to determine the value of each delay associated with each LD unit (relative to the start of the frame) is equal to 1 ms (based on typical processor speeds) then our delay adaptation method set up or training time is 72 ms (9 RGB-LDs in each unit × 8 light units × 1 ms). This training rate (once every 1second frame) is sufficient given that the delay adaptation has to be carried out at the rate at which the environment changes (pedestrian movement). Therefore, the adaptive system can achieve 100% of the specified data rate when it is stationary, and 92.8% in the case of typical user movement, i.e., 10 Gbps when it is stationary and 9.3 Gbps when there are environmental changes (user or object movement in the room). The medium access control (MAC) protocol used to share the VLC medium between users should include a repetitive training period to perform the beam delay adaptation. The design of the MAC protocol is not considered in this work. Our delay adaptation algorithm has been considered at one given receiver location in a single user scenario. In the case of a multiuser scenario, scheduling [49] can be used where the delay adaptation algorithm is chosen to maximise the 3 dB channel bandwidth and the SNR in a given region for a given time period. The delay adaptation can be implemented through delayed switching of the VLC sources.

It should be noted that the RGB-LD light units (i.e. eight transmitters) should always be 'ON' to provide illumination for the room. Therefore, to prevent flickering, an OOK dimming technique may be used [50].

VII. SIMULATION RESULTS AND DISCUSSION OF THE DELAY ADAPTION TECHNIQUE

We evaluated the performance of the delay adaptation technique in the presence of multipath propagation, ISI and mobility for the two VLC systems in an empty room. The results of the imaging LD-VLC system are compared with those of the DAT imaging LD-VLC system. The results are presented in terms of impulse response, delay spread, 3 dB channel bandwidth and SNR.

A. Impulse Responses

The impulse responses of the imaging LD-VLC and DAT imaging LD-VLC at the room centre (worst case scenario) are depicted in Fig.12. At the room centre the distance between the transmitter and receiver becomes maximum which leads to increase in delay spread, path loss and decrease in SNR. Therefore, the location ((2m, 4m, 1m), room centre) is the worst case scenario. The LOS components have a great impact on the system performance. Therefore, we magnified the impulse response for these systems to show the LOS clearly. It can be seen that the DAT imaging system impulse response is better than the imaging system in terms of signal spread. By reducing the signal spread, this leads to an increase in the 3 dB channel bandwidth which decreases the multipath induced ISI and enables higher throughput for the VLC system.
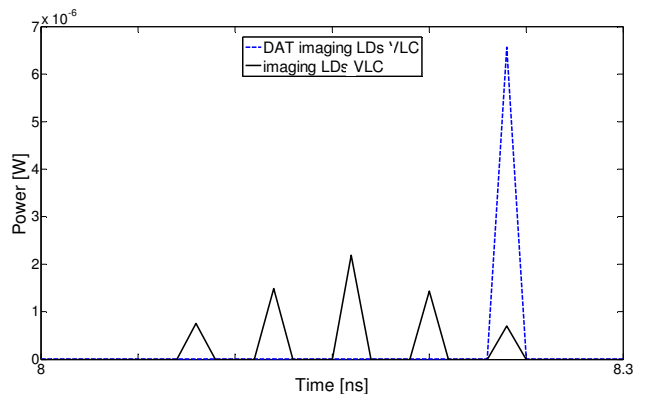

Fig.12: Impulse responses of the two systems at room centre (2m, 4m, 1m).

B. Delay Spread Performance

Fig.13 presents the SB delay spread performance of the imaging and DAT imaging systems in a worst case scenario (when the receiver moves along the line x=2m). The results show that the DAT imaging LD-VLC system outperforms the imaging LD-VLC system by decreasing the delay spread by a factor of 6, from 0.04 ns to 0.007 ns at the room centre. Although, the MRC resulted in the best SNR (see Figs. 10 and 11) compared to SB, it should be noted that it has a slightly higher delay spread. This increase is attributed to some pixels that collect only reflection components (without LOS) which leads to an increase in delay spread. Overall, this increase in delay spread is not high and can be acceptable noting that MRC results in improved SNR.
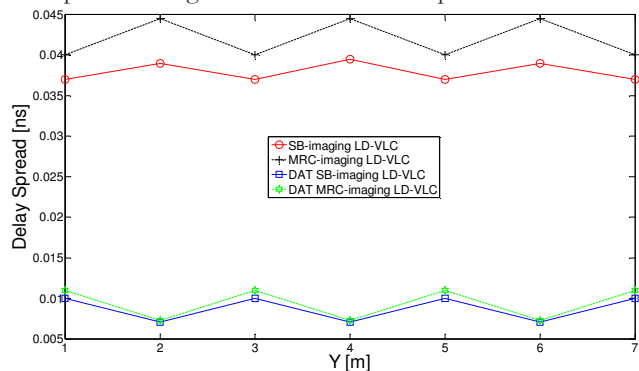

Fig.13: SB and MRC delay spread of the two systems at x=2m and along y-axis.

C. 3 dB Channel Bandwidth

The 3 dB channel bandwidth of the two systems (i.e. imaging LD-VLC and DAT imaging LD-VLC) when the receiver moves along the x=2m line is given in Table I. The results show that the DAT imaging LD-VLC system offers 3 dB channel bandwidth of more than 16 GHz in the worst case in the rooms examined (which are of typical size), which is the highest channel bandwidth reported for a VLC system to the best of our knowledge. The significant increase in channel bandwidth enables our proposed systems to operate at higher data rates. For example, a 10 Gbps data rate requires a 7 GHz channel bandwidth with simple OOK modulation, our new adaptive systems can achieve higher data rates [43].

TABLE I
CHANNEL BANDWIDTH OF THE PROPOSED SYSTEMS

System	3 dB channel Bandwidth [GHz]						
	Receiver Locations along the y-axis, Y [m]						
	1	2	3	4	5	6	7
Imaging LD-VLC	5.2	4.19	5.2	4.19	5.2	4.19	5.2
DAT Imaging LD-VLC	16.6	23.4	16.6	23.4	16.6	23.4	16.6

9

D. SNR Performance

Fig.14 illustrates the SNR (SB and MRC) of the imaging and DAT imaging systems when operating at 30 Mbps. It is observed that the DAT system does not give any advantage over the imaging system at low data rates due to the high channel bandwidth achieved by the imaging system (i.e. 4.2 GHz), which guarantees low ISI at the low operating bit rate considered (30 Mbps).

Fig.15 shows the SNR of the imaging and DAT imaging systems at a high data rate (10 Gbps). These results show that the SNR fluctuations in the imaging system at high data rates are reduced and the SNR is improved by 6 dB when using MRC combing (BER better than 10^{-5}) in the DAT imaging system. The DAT imaging system has the ability to achieve more than 23 Gbps (16 GHz channel bandwidth is achieved). Forward error correction codes (FEC) can be used to further reduce the BER form 10^{-5} to 10^{-9} in this proposed DAT imaging LD-VLC system.
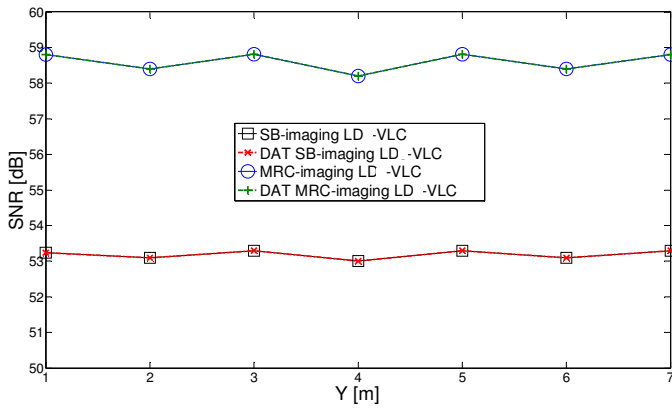

Fig.14: SNR of imaging system and DAT imaging system when both operate at 30 Mbps, when the receivers move at x=2m and along y-axis.
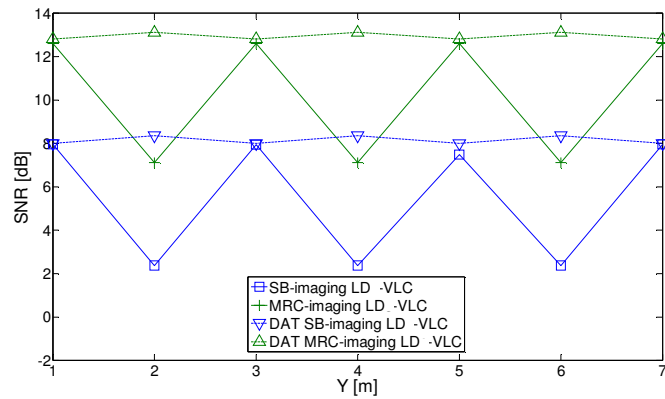

Fig.15: SNR of imaging system and DAT imaging system when both operate at 10 Gbps, when the receivers move at x=2m and along y-axis.

VIII. ROBUSTNESS TO SHADOWING AND SIGNAL BLOCKAGE

We extended the analysis and evaluation of the performance of the proposed system (i.e. DAT imaging LD-VLC system) to a realistic room environment with mobility. In this realistic environment, signal blockage (as a result of cubicles), a door, windows, furniture, multipath propagation and mobility are all present. To evaluate the effect of signal blockage, mobility and shadowing on the VLC communication link, we considered the room shown in Fig.1 (b). The results of the DAT system was compared in rooms A (an empty room) and B (realistic room) in terms of impulse response, path loss, delay spread and SNR. We have considered a mobile user with a speed of 1 m/s moving along the y-axis in the lines x=1m or x=2m, the results in this Section are presented in two places in the room 1) when the user is inside a mini cubicles (x=1m and along y-axis) and 2) when

the mobile user is in the middle of the room (x=2m and along y-axis). In this Section a simulation package based on a ray-tracing algorithm was developed using MATLAB to compute the impulse response of the DAT imaging LD-VLC system in a realistic environment. Additional features were introduced for a realistic room. In the realistic environment for each receiver location the first step is to check the availability of LOS component (certain conditions were introduced to the simulator to check the existence of LOS, 1st and 2nd order reflection components in each location) then the received power due to 1st and 2nd order reflections is also calculated.

A. Impulse Responses

Channel impulse responses at the room centre (i.e. x=2m and y=4m) for the DAT imaging system are shown in Fig.16 for rooms A and B. It should be noted that both impulse responses of the proposed system are dominated by short initial impulses due to the LOS path between transmitter and receiver. In addition, it can be clearly seen that the proposed system has good robustness against shadowing and mobility, and it has the ability to maintain LOS even in this harsh environment (i.e. room B), which is attributed to the number of transmitters that are distributed on the ceiling (i.e. eight RGB LDs light units). However, the amount of received optical power from the reflections in room B is less than that received in room A, as shown in Fig.16, and this is because of the existence of the door, windows, cubicles, partitions and bookshelves in room B that lead to reduced multipath propagation. Although the received power from reflections was severely affected in room B, the LOS component remained the same in both room configurations in both systems, and the LOS component has the largest impact on the system performance. For example, the received optical power associated with the DAT imaging LD-VLC system in room A was 6.69 μW, whereas it was 6.63 μW in room B, which indicates that the reduction in power is negligible (the reduction in power was 0.063 μW).
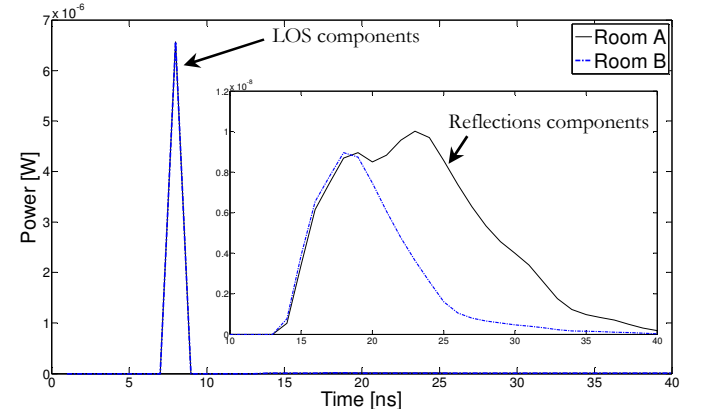

Fig.16: Impulse responses of DAT imaging system at room centre (2m, 4m, 1m) in two different environments (rooms A and B).

B. Path Loss

The main target of any communication system is to achieve high SNR or low BER at the receiver side. The SNR in OW systems is based mainly on the square of the received optical signal power [28]. Therefore, the average received optical power and path loss explain part of the main VLC system performance in the two different environments. Optical path loss can be defined as [51]:

$$PL(dB) = -10log_{10}(\int h(t)dt) \tag{18}$$

where $h(t)$ is the system impulse response. Fig.17 illustrates the optical path loss of the DAT imaging system in rooms A and B. It

is observed that the performance of the proposed system is comparable in rooms A and B, and this can be attributed to the LOS links available on the entire CF, which protects against shadowing and mobility in this system. It can be noticed that the path loss can be higher when the receiver moves along x=2m. This is due to the larger distance between the receiver and transmitter. Overall, the proposed systems were evaluated and it was shown that they are able to achieve similar performance levels in an empty room and in a realistic indoor environment.
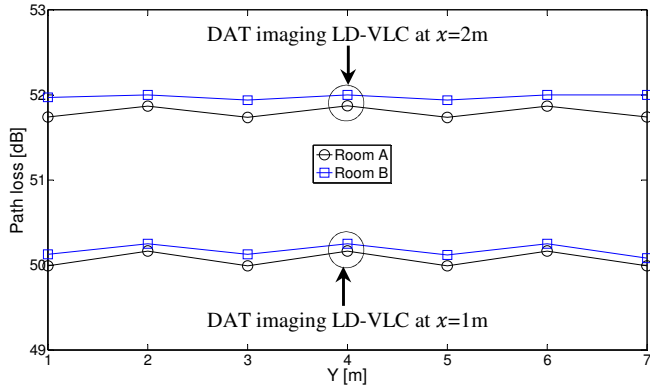

Fig.17: Optical path loss distribution of the DAT imaging system in two different environments (rooms A and B) at x=1m and x=2m along y-axis.

C. Delay Spread Analysis

Fig.18 shows the delay spread of the DAT system in two different environments (i.e. rooms A and B). It can be clearly seen that the DAT imaging system has lower delay spreads in room B than in room A, and this is attributed to two reasons: firstly, the proposed system has the ability to establish a LOS link at all receiver positions. Secondly, reflections from the door and windows are set to zero, while the other two walls in room B are covered by filling cabinets and bookshelves with a small diffuse reflectivity of 0.4. This means that the power contribution from the reflections is minimal and this reduced the delay spread. The non-symmetry in the delay spread curve in room B is due to the presence of windows at one end of the room and the presence of bookshelves at the other end. In room B, when the receiver position was close to the windows, for example, at points (x=1m and y=1m) and (x=2m and y=1m) the delay spread becomes very low because the received power from the reflections is very low. However, when the receiver moves towards the other side of the room (i.e. receiver positions close to bookshelves), for instance, at points (x=1m and y=7m) and (x=2m and y=7m), the delay spread increases due to the power received from the signals reflected by the bookshelves.

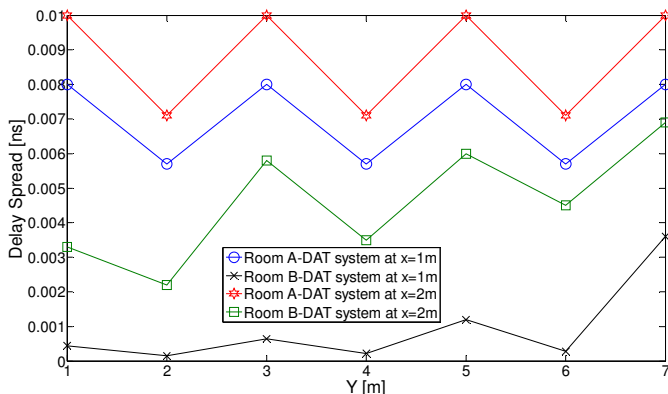Fig.18: Delay spread of DAT imaging system in two different environments (rooms A and B) at x=1m and at x=2m and along y-axis.

D. 3 dB channel bandwidth

The 3 dB channel bandwidth of the DAT imaging LD-VLC in two different environments (rooms A and B) when the receiver moves along the x=2m line is given in Table II. The results show that the DAT imaging LD-VLC system offers 3 dB channel bandwidth of more than 24 GHz in room B. Therefore, room B outperforms room A in terms of 3 dB channel bandwidth as the delay spread decreased in room B (see Fig.18).

TABLE II
CHANNEL BANDWIDTH OF THE DAT IMAGING LD-VLC IN TWO DIFFERENT ENVIRONMENTS

DAT Imaging LD-VLC	3 dB channel Bandwidth [GHz]						
	Receiver locations along the y-axis, Y [m]						
	1	2	3	4	5	6	7
Room A	16.6	23.4	16.6	23.4	16.6	23.4	16.6
Room B	37.1	38.9	28.7	36.7	27.7	31.6	24.1

E. SNR Performance

Fig.19 shows the SB-SNR results against receiver location for the DAT system in two room scenarios. The DAT imaging system has a slightly lower SNR in Room B and this due to the reduction in received power. It should be noted that the results in Fig.19 are in agreement with the general observation made in Fig.17. For instance, the DAT system in room B has a path loss higher than that in room A which leads to a decrease in SNR.
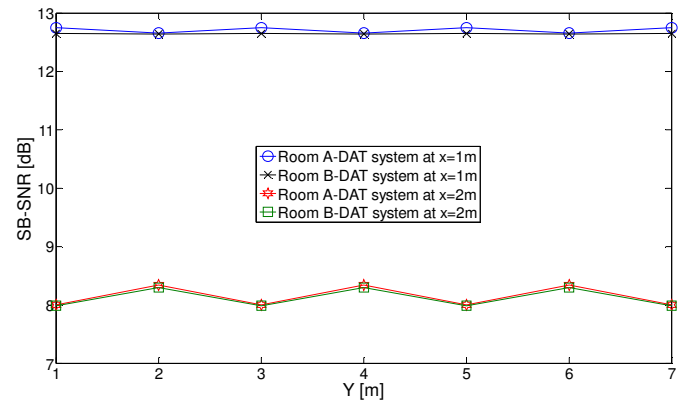

Fig.19: SB-SNR of DAT system in two different environments (rooms A and B) when system operated at 10 Gbps at x=1m and at x=2m and along y-axis.

IX. CONCLUSIONS

To summarise, we proposed, designed and investigated a novel LD-VLC system that uses LDs instead of LEDs as the transmitters in conjunction with two different receivers (wide-FOV receiver and an imaging receiver) to deal with the main constraints of the traditional VLC system, namely the low modulation bandwidth of the LEDs and ISI caused by multipath dispersion. To the best of our knowledge, the data rates achieved by our proposed systems (i.e. 5 Gbps with the imaging LD-VLC system and 10 Gbps with the DAT imaging LD-VLC system) are the highest data rates to date for an indoor mobile VLC system with simple modulation format and without the use of relatively complex wavelength division multiplexing approaches.

A novel delay adaptation technique was introduced for a VLC system and imaging receivers were used to improve the SNR and channel bandwidth as well as to reduce the effect of multipath dispersion. In addition, our proposed system was evaluated in a harsh environment with mobility, and the results showed that our system is robust in the presence of shadowing and mobility.

11

Our imaging LD-VLC system has the ability to decrease the delay spread of the wide FOV LD-VLC system by 94% from 0.7 ns to 0.04 ns at the room centre (x=2m and y=4m), which leads to an increase in the channel bandwidth by a factor of 36 from 116 MHz to 4.2 GHz.

In addition, at a low data rate (30 Mbps) our proposed system (imaging LD-VLC) offers SNR improvement of 8 dB, and the lowest SNR achieved was 19.2 dB at a high data rate (5 Gbps) at the room centre. Moreover, our imaging LD-VLC system employs an OOK modulation scheme that adds simplicity to the VLC system. Our system provides full mobility within the test area in the presence of multipath propagation and achieves a BER better than 10^{-9} at 5 Gbps.

The DAT imaging LD-VLC system has the ability to decrease the delay spread of the imaging LD-VLC system by 83% from 0.04 ns to 0.007 ns at the room centre, which leads to an increase in the channel bandwidth by a factor of 5.4 from 4.2 GHz to 23 GHz, and this channel bandwidth has the ability to provide data rates of up to 33 Gbps. Moreover, at low data rates (30 Mbps), the proposed algorithm does not offer SNR improvements, which is due to the low ISI at these data rates. The BER provided by our DAT imaging system is better than 10^{-5} at 10 Gbps, in the worst case scenarios. The DAT imaging system in a realistic room has lower delay spread (higher 3 dB channel bandwidth) but also lower received power and overall has slightly lower SNR.

Future work will address methods to enhance the SNR of the DAT imaging LD-VLC system to achieve data rates higher than 10 Gbps.

REFERENCES

[1] D. O'Brien, G. Parry, and P. Stavrinou, "*Optical hotspots speed up wireless communicatio,*" Nature Photonics, vol.1, no.5, pp.245-247, 2007.

[2] A. T. Hussein, and J. M. H. Elmirghani, "*A Survey of Optical and Terahertz (THz) Wireless Communication Systems,*" IEEE Communications Surveys & Tutorials, (to be submitted), 2015.

[3] H. L. Minh, D. C. O Brien , G. Faulkner , L. Zeng , K. Lee , D. Jung and Y. Oh, "*80 Mbit/s visible light communications using pre-equalized white LED,*" in Proc. 34th European Conference on Optical Communication (ECOC), pp.1 -2, 2008.

[4] A. M. Khalid, G. Cossu, R. Corsini, P. Choudhury, E. Ciaramella, "*1-Gb/s transmission over a phosphorescent white LED by using rateadaptive discrete multitone modulation,*" IEEE Photonics Journal, vol.4, issue 5, pp.1465-1473, 2012.

[5] G. Cossu, A. M. Khalid, P. Choudhury, R. Corsini, and E. Ciaramella, "*3.4 Gbit/s visible optical wireless transmission based on RGB LED,*" Optics express, vol.20, no.26, pp.501-506, 2012.

[6] Z. Xie, K. Cui, H. Zhang, and Z. Xu, "*Capacity of MIMO visible light communication channels,*" In Photonics Society Summer Topical Meeting Series, pp.159-160, 2012.

[7] P. A. Haigh, T. T. Son, E. Bentley, Z. Ghassemlooy, H. Le Minh and L. Chao, "*Development of a Visible Light Communications System for Optical Wireless Local Area Networks,*" in Proc. IEEE Computing, Communications and Applications Conference (ComComAp), pp.315-355, 2012.

[8] H. L. Minh, D. C. O Brien , G. Faulkner , L. Zeng , K. Lee , D. Jung and Y. Oh , "*High-speed visible light communications using multiple-resonant equalization,*" IEEE Photon Technol Letter, vol.20, no.14, pp.1243 -1245 2008.

[9] L. Zeng, H. L. Minh, D. C. O Brien, G. Faulkner, K. Lee, D. Jung, Y. Oh, "*Equalisation for high-speed Visible Light Communications using white-LEDs,*" in Proc. 6th International Symposium on Communication Systems, Networks and Digital Signal Processing (CNSDSP), pp170–173, 2008.

[10] K. D. Langer, J. Vucic, C. Kottke, L. Fernandez, K. Habel, A. Paraskevopoulos, M. Wendl and V. Markov, "*Exploring the potentials of optical-wireless communication using white LEDs,*" 13th International Conference on Transparent Optical Networks (ICTON), pp.1-5, June 2011.

[11] C. Kottke, J. Hilt, K. Habel, J. Vučić, and K. Langer, "*1.25 Gbit/s visible light WDM link based on DMT modulation of a single RGB LED luminary,*" In European Conference and Exhibition on Optical Communication, pp. We-3, Optical Society of America, 2012.

[12] S. Zhang, S. Watson, J. McKendry, D. Massoubre, A. Cogman, R. K. Henderson, A. E. Kelly, and M. D. Dawson, "*1.5 Gbit/s multi-channel visible light communications using CMOS-controlled GaN-based LEDs,*" Journal of Lightwave Technology, vol.31, no.8, pp.1211-1216, 2013.

[13] N. Fujimoto, and H. Mochizuki, "*477Mbit/s Visible Light Transmission Based on OOK-NRZ Modulation Using A Single Commercially Available Visible LED and a Practical LED Driver with a Pre-Emphasis Circuit,*" Optical Fibre Communication Conference and Exposition and the National Fibre Optic Engineers Conference (OFC/NFOEC), pp1-3, 2013.

[14] D. Tsonev, H. Chun, S. Rajbhandari, J. McKendry, S. Videv, E. Gu, M. Haji, S. Watson, A. Kelly, G. Faulkner, M. Dawson, H. Haas, and D. O'Brien, "*A 3-Gb/s Single-LED OFDM-Based Wireless VLC Link Using a Gallium Nitride µLED,*" IEEE Photon. Technol. Lett., vol. 26, no.7, pp.637–640, 2014.

[15] "*Laser Light Leading the Way to the Future,*" [online] Available: http://46.4.5.252/en_au/bmw-i8/laser-light-leading-the-way-to-the-future/94/laser-light-leading-the-way-to-the-future. Last access on 01/02/2015.

[16] A. Neumann, J. J. Wierer, W. Davis, Y. Ohno, S. Brueck, and J. Y. Tsao. "*Four-color laser white illuminant demonstrating high color-rendering quality,*" Optics express, vol.19, no.104, pp.982-990, 2011.

[17] R. Gatdula, J. Murray, A. Heizler, and M. Shah, "*Solid State Lighting with Blue Laser Diodes,*" [online] Available: http://www.winlab.rutgers.edu/~crose/capstone12/entries/SolidStateLightingwBlueLaserDiodes-Revised.pdf. Last access on 01/02/2015.

[18] C. Basu, M. Meinhardt-Wollweber, and B. Roth, "*Lighting with laser diode,*"Advanced Optical Technologies, vol.2, issue 4, pp. 313-321, 2013.

[19] "*LD Lighting Engine is a new type of light source from Toshiba,*" [online] Available: http://reefbuilders.com/2012/07/23/ld-lighting-engine-toshiba/. Last access on 01/02/2015.

[20] K. A. Denault, M. Cantore, S. Nakamura, S. P. DenBaars, and R. Seshadri, "*Efficient and stable laser-driven white lighting,*" AIP Advances, vol.3, no.7, pp. 2013.

[21] Y. Tanaka, T. Komine, S. Haruyama, and M. Nakagawa, "*Indoor visible communication utilizing plural white LEDs as lighting,*" International Symposium 12th IEEE in Personal, Indoor and Mobile Radio Communications, vol.2, pp.81-85, 2001.

[22] N. Saha, R. K. Mondal, N. T. Le, and Y. M. Jang, "*Mitigation of interference using OFDM in visible light communication,*" International Conference on ICT Convergence (ICTC), pp.159-162, 2012.

[23] K. K. Wong and T. O'Farrell, "*Spread spectrum techniques for indoor wireless IR communications',*" IEEE Wireless Communications, vol.10, no.2, pp.54-63, 2003.

[24] Z. Wang, C. Yu, W. Zhong, J. Chen and W. Chen , "*Performance of a novel LED lamp arrangement to reduce SNR fluctuation for multi-user visible light communication systems,*" Optics Express, vol.20, no.4, pp.4564-4573, 2012.

[25] "*European standard EN 12464-1: Lighting of indoor work places,*" [online] Available:http://www.etaplighting.com/uploadedFiles/Downloadable_documentation/documentatie/EN12464_E_OK.pdf. Last access on 01/02/2015.

[26] W. R.McCluney, "*Introduction to radiometry and photometry",* Artech House, 1994.

[27] A. Ryer and V. Light, "*Light measurement handbook,*" [online] Availaable: http://irtel.uni-mannheim.de/lehre/seminar-psychophysik/artikel/Alex_Ryer_Light_Measurement_Handbook.pdf. Last access on 01/02/2015.

[28] J. M. Kahn and J. R. Barry, "*Wireless infrared communications,*" Proc. IEEE, vol.85, no.2, pp. 265-298, 1997.

[29] T. Komine and M. Nakagawa, "*Fundamental analysis for visible-light communication system using LED lights,*" IEEE Transactions on Consumer Electronics, vol.50, no.1, pp.100-107, 2004.

[30] T. Komine "*Visible Light Wireless Communication and Its Fundamental,*" PhD thesis in Department of Information and Computer Science, Keio University, 2005.

[31] F. R. Gfeller, and U. H. Bapst, "*Wireless in-house data communication via diffuse infrared radiation,*" Proc. IEEE, vol. 67, no.11, pp. 1474-1486, 1979.

[32] F. E. Alsaadi, M.A. Alhartomi, and J.M.H. Elmirghani, "*Fast and Efficient Adaptation Algorithms for Multi-Gigabit Wireless Infrared Systems,*" Journal of Lightwave Technology, vol.31, no.23, pp.3735-3751, 2013.

[33] J. R. Barry, J. M. Kahn, W. J. Krause, E. A. Lee, and D. G. Messerschmitt, "*Simulation of multipath impulse response for indoor wireless optical channels ,*" IEEE Journal Selected Areas Communication, vol.11, no.3, pp.367-379 , 1993.

[34] S. Soltic, and A. Chalmers, "*Optimization of laser-based white light illuminants,*" Optics express, vol.21, no.7, pp.8964-8971, 2013.

[35] A. Stimson, "*Photometry and radiometry for engineers,*" New York, Wiley-Interscience, 1974.

[36] M. Biagi, T. Borogovac, and T.D.C. Little, "*Adaptive Receiver for Indoor Visible Light Communications,*"Journal of Lightwave Technology, vol.31, no.23, pp.3676-3686, 2013.

[37] A. G. Al-Ghamdi and J. M. H. Elmirghani, "*Line strip spot-diffusing transmitter configuration for optical wireless systems influenced by background noise and multipath dispersion,*" IEEE Transactions Communication, vol.52, no.1, pp.37-45, 2004.

[38] P. Djahani and J. M. Kahn, "*Analysis of Infrared Wireless Links Employing Multibeam Transmitter and Imaging Diversity Receivers,*" IEEE Transactions Communication, vol.48, no.12, pp.2077-2088, 2000.

[39] A. G. Al-Ghamdi, and J.M.H. Elmirghani, "*Analysis of diffuse optical wireless channels employing spot-diffusing techniques, diversity receivers, and combining schemes,*" IEEE Transactions on Communications, vol.52, no.10, pp.1622-1631, 2004.

[40] F. E. Alsaadi, and J. M. H. Elmirghani, "*High-speed spot diffusing mobile optical wireless system employing beam angle and power adaptation and imaging receivers,*" Journal of Lightwave Technology, vol.28, no.16, pp.2191–2206, 2010.

[41] J. M. Kahn, P. Djahani, A. G. Weisbin, B. K. Teik and A. Tang, "*Imaging diversity receivers for high-speed infrared wireless communication,*" IEEE Communications Magazine, vol.36, no.12, pp.88-94, 1998.

[42] F. E. Alsaadi, and J.M.H. Elmirghani, "*Mobile Multigigabit Indoor Optical Wireless Systems Employing Multibeam Power Adaptation and Imaging Diversity Receivers,*" IEEE Journal of Optical Communications and Networking, vol.3, no.1, pp.27-39, 2011.

[43] S. D. Personick, "*Receiver design for digital fiber optical communication system, Part I and II*", Bell System Technology Journal, vol.52, no. 6, pp 843-886, 1973.

[44] M. T. Alresheedi, and J.M.H. Elmirghani, "*10 Gb/s Indoor Optical Wireless Systems Employing Beam Delay, Power, and Angle Adaptation Methods With 'Imaging Detection,*" Journal of Lightwave Technology, vol.30, no.12, pp.1843-1856, 2012.

[45] J.M.H. Elmirghani, H. Chan, and R. Cryan, "*Sensitivity evaluation of optical wireless PPM systems utilising PIN-BJT receivers,*" IEE Proceedings-Optoelectronics, vol.143, no.6, pp.355-359, 1996.

[46] B. Leskovar, "*Optical receivers for wide band data transmission systems,*" IEEE Transactions on Nuclear Science, vol.36, no.1, pp.787-793, 1989.

[47] E. M. Kimber, B. L. Patel, I. Hardcastle, and A. Hadjifotiou, "*High performance 10 Gbit/s pin-FET optical receiver,*" Electronics Letters, vol.28, no.2, pp.120-122, 1992.

[48] M. Tolstrup, "*Indoor Radio Planning: A Practical Guide for Gsm, Dcs, Umts, Hspa and Lte,*" John Wiley & Sons., 2011.

[49] P. Viswanath, D. N. C. Tse, and R. Laroia, "*Opportunistic beamforming using dumb antennas,*" IEEE Transactions on Information Theory, vol.48, no.6 pp.1277-1294, 2002.

[50] "*IEEE Standard for Local and Metropolitan Area Networks-Part 15.7: Short-Range Wireless Optical Communication Using Visible Light,*" pp.1-309, 2011.

[51] A. G. Al-Ghamdi, and J.M.H. Elmirghani, "*Performance comparison of LSMS and conventional diffuse and hybrid optical wireless techniques in a real indoor environment,*" IEE Proceedings Optoelectronics, vol.152, issue.4, pp.230-238, 2005.

Ahmed Taha Hussein received a B.Sc. (First Class Hons.) in the Electronic and Electrical Engineering from the University of Mosul, Iraq, in 2006 and an M.Sc. degree (with distinction) in communication systems from the University of Mosul, Iraq, in 2011. He is a Higher Committee for Education Developments in Iraq (HCED) Scholar and is currently working toward a Ph.D. degree in the School of Electronic and Electrical Engineering, University of Leeds, Leeds, UK.

  Prior to his Ph.D. study, he worked as a Communication Instructor in Electronic and Electrical Engineering Department in the College of Engineering, University of Mosul, Iraq from 2006 to 2009. He also worked as a lecturer in the Electronic and Electrical Engineering Department in the College of Engineering, University of Mosul, Iraq from 2011 to 2012. His research interests include performance enhancement techniques for visible light communication systems, visible light communication system design and indoor visible light communication networking.

Prof. Jaafar M. H. Elmirghani is the Director of the Institute of Integrated Information Systems within the School of Electronic and Electrical Engineering, University of Leeds, UK. He joined Leeds in 2007 and prior to that (2000–2007) as chair in optical communications at the University of Wales Swansea he founded, developed and directed the Institute of Advanced Telecommunications and the Technium Digital (TD), a technology incubator/spin-off hub. He has provided outstanding leadership in a number of large research projects at the IAT and TD. He received the Ph.D. in the synchronization of optical systems and optical receiver design from the University of Huddersfield UK in 1994 and the DSc in Communication Systems and Networks from University of Leeds, UK, in 2014. He has co-authored Photonic switching Technology: Systems and Networks, (Wiley) and has published over 400 papers. He has research interests in optical systems and networks. Prof. Elmirghani is Fellow of the IET, Fellow of the Institute of Physics and Senior Member of IEEE. He was Chairman of IEEE Comsoc Transmission Access and Optical Systems technical committee and was Chairman of IEEE Comsoc Signal Processing and Communications Electronics technical committee, and an editor of IEEE Communications Magazine. He was founding Chair of the Advanced Signal Processing for Communication Symposium which started at IEEE GLOBECOM'99 and has continued since at every ICC and GLOBECOM. Prof. Elmirghani was also founding Chair of the first IEEE ICC/GLOBECOM optical symposium at GLOBECOM'00, the Future Photonic Network Technologies, Architectures and Protocols Symposium. He chaired this Symposium, which continues to date under different names. He was the founding chair of the first Green Track at ICC/GLOBECOM at GLOBECOM 2011, and is Chair of the IEEE Green ICT committee within the IEEE Technical Activities Board (TAB) Future Directions Committee (FDC), a pan IEEE Societies committee responsible for Green ICT activities across IEEE, 2012-2015. He is and has been on the technical program committee of 33 IEEE ICC/GLOBECOM conferences between 1995 and 2014 including 14 times as Symposium Chair. He received the IEEE Communications Society Hal Sobol award, the IEEE Comsoc Chapter Achievement award for excellence in chapter activities (both in 2005), the University of Wales Swansea Outstanding Research Achievement Award, 2006, the IEEE Communications Society Signal Processing and Communication Electronics outstanding service award, 2009 and a best paper award at IEEE ICC'2013. He is currently an editor of: IET Optoelectronics, Journal of Optical Communications, IEEE Communications Surveys and Tutorials and IEEE Journal on Selected Areas in Communications series on Green Communications and Networking. He is Co-Chair of the GreenTouch Wired, Core and Access Networks Working Group, an adviser to the Commonwealth Scholarship Commission, member of the Royal Society International Joint Projects Panel and member of the Engineering and Physical Sciences Research Council (EPSRC) College. He has been awarded in excess of £22 million in grants to date from EPSRC, the EU and industry and has held prestigious fellowships funded by the Royal Society and by BT. He is an IEEE Comsoc Distinguished Lecturer 2013-2016.